Geophysical Research Letters

RESEARCH LETTER
10.1029/2019GL083235

U.S. Hydrologic Design Standards Insufficient Due to Large Increases in Frequency of Rainfall Extremes

Daniel B. Wright[1], **Christopher D. Bosma**[1], **and Tania Lopez-Cantu**[2]

[1]Department of Civil and Environmental Engineering, University of Wisconsin-Madison, Madison, WI, USA, [2]Department of Civil and Environmental Engineering, Carnegie Mellon University, Pittsburgh, PA, USA

Key Points:
- Conventional analyses neglect trends in extreme rainfall events such as the 100-year storm, which are critical for engineering design
- A regional aggregation approach reveals significant trends in very extreme rainfall in the United States, mainly due to climate warming
- Existing hydrologic infrastructure and analyses in much of the United States may be underperforming due to increases in storm activity

Supporting Information:
- Supporting Information S1

Correspondence to:
D. B. Wright,
danielb.wright@wisc.edu

Citation:
Wright, D. B., Bosma, C. D., & Lopez-Cantu, T. (2019). U.S. hydrologic design standards insufficient due to large increases in frequency of rainfall extremes. *Geophysical Research Letters*, *46*. https://doi.org/10.1029/2019GL083235

Received 8 APR 2019
Accepted 8 JUL 2019
Accepted article online 12 JUL 2019

Abstract Evidence for intensifying rainfall extremes has not translated into "actionable" information needed by engineers and risk analysts, who are often concerned with very rare events such as "100-year storms." Low signal-to-noise associated with such events makes trend detection nearly impossible using conventional methods. We use a regional aggregation approach to boost this signal-to-noise, showing that such storms have increased in frequency over much of the conterminous United States since 1950, a period characterized by widespread hydrologic infrastructure development. Most of these increases can be attributed to secular climate change rather than climate variability, and we demonstrate potentially serious implications for the reliability of existing and planned hydrologic infrastructure and analyses. Though trends in rainfall extremes have not yet translated into observable increases in flood risks, these results nonetheless point to the need for prompt updating of hydrologic design standards, taking into consideration recent changes in extreme rainfall properties.

Plain Language Summary Numerous studies have shown that heavy rainfall in the United States and elsewhere is becoming more common and more severe in a warming climate. These studies have not shown, however, how the most extreme rainfall events are changing, since these storms are so rare that they are difficult to assess using conventional techniques, which generally focus on changes at individual geographic locations. We instead use a simple aggregation technique to "pool" multiple observations within a region. This "pooling" allows us to show that rainfall events that exceed common engineering design criteria, including 100-year storms, have increased in frequency in most parts of the United States since 1950—a period of widespread infrastructure construction. We show that in most locations, these increases are likely due to climate warming. We also show that much of the existing and planned hydrologic infrastructure in the United States based on published rainfall design standards is and will continue to underperform its intended reliability due to these rainfall changes.

1. Introduction

Statistical distributions of extreme rainfall, referred to as intensity-duration-frequency (IDF) relationships or "curves," have long been used in hydrologic infrastructure design and floodplain mapping. Such applications often consider impacts that would result from, for example, the "100-year storm," a hypothetical rainfall depth or intensity said to have a "100-year annual recurrence interval (ARI)," corresponding to a 1% annual exceedance probability. IDF relationships corresponding to short rainfall durations are often used to characterize flood responses in the small watersheds that are most sensitive to short-lived storms; longer-duration IDFs are used for the design of larger infrastructure such as reservoirs. Commonly used IDF standards in the United States and elsewhere do not account for potential rainfall nonstationarity (i.e., change over time; Milly et al., 2008), while many existing hydrologic structures and studies are based on IDF standards developed using data records ending in the 1960s. Thus, if the properties of extreme rainfall have changed in recent decades, these IDF standards and the hydrologic designs based upon them may be unreliable now or in the future.

The number and magnitude of extreme rainfall events are indeed increasing in many parts of the United States and worldwide (e.g., Feng et al., 2016; Guilbert et al., 2015; Kunkel et al., 1999; Kunkel et al., 2012; Powell & Keim, 2014), likely attributable to increases in atmospheric water vapor associated with anthropogenic warming. Climate models project continued trends into the foreseeable future (Easterling et al., 2017; Field et al., 2012). There has been a failure, however, to translate evidence for rainfall nonstationarity into "actionable" (i.e., specific quantitative) information for hydrologic design and

analysis. Indeed, common definitions of "extreme" used in most trend studies correspond to smaller and more frequent events than the 10- to 500-year ARIs that are of interest in many hydrologic applications (Bonnin, Maitaria, & Yekta, 2011; Hodgkins et al., 2017; Seneviratne et al., 2012). A chief reason for this failure is that assessing quantitative changes in very rare events is extremely difficult compared with more frequent storms: consider a rain gage with a century-long observational record—in a stationary climate, one 100-year exceedance is expected on average. (The probability of exactly one exceedance in 100 years is approximately 0.370 via the binomial distribution; the probabilities of zero, two, and three such exceedances are 0.366, 0.185, and 0.061, respectively.) Even for records with several exceedances, the low signal-to-noise makes it impossible to identify a clear trend. Thus, even though several statistical methods exist that can generate nonstationary IDF estimates (e.g., Cheng & AghaKouchak, 2014; Gilleland & Katz, 2016), the statistical uncertainties for long ARI events such as the 100-year storm are very large (Serinaldi & Kilsby, 2015), which likely explains why such methods have yet to be widely adopted in practice.

In this study, we use a regional aggregation approach to boost the signal-to-noise ratio to detect trends in the frequency of rainfall totals exceeding commonly used IDF standards. We also examine potential causes for such trends, and, unlike previous studies, we explore potential implications for the reliability of hydrologic infrastructure and analyses.

2. Data and Methods

2.1. IDF Estimates

Under the Atlas 14 project (Bonnin et al., 2006), the National Oceanic and Atmospheric Administration (NOAA) has produced stationary IDF estimates (means and 90% confidence intervals [CIs]) for a range of ARIs (up to 1,000 years) and durations for most of the conterminous United States (CONUS). The Atlas 14 methodology utilizes regionalized L-moments (Bonnin et al., 2006, Bonnin, Martin, et al., 2011; Hosking & Wallis, 2005; Perica et al., 2014, 2013b, 2013a), which use extreme rainfall observations from within a "homogeneous region" (i.e., an area within which rainfall extremes are relatively homogeneous) to generate IDF estimates at individual locations. Once a homogeneous region is identified, a statistical distribution is chosen that adequately fits the observations of rainfall extremes in this region. Distributions considered in Atlas 14 include the Generalized Logistic, Generalized Extreme Value, Generalized Normal, Generalized Pareto, and Pearson Type III. Multiple goodness-of-fit measures, including Monte Carlo simulation, "real data checks," and L-moment errors, are used for distribution selection.

The earliest Atlas 14 estimates appeared for the Ohio River basin and surrounding areas in 2004 (Bonnin et al., 2006). Estimates have yet to be produced for Washington, Oregon, Idaho, Montana, and Wyoming, which are thus omitted from our study. Lopez-Cantu and Samaras (2018) provide a detailed timeline of Atlas 14 up to late 2017 (estimates for Texas were published in 2018; Perica et al., 2018). Atlas 14 is currently the most reliable and widely used source of IDF estimates in the United States. Technical Paper 40 (TP40; Hershfield, 1961) was the predecessor to Atlas 14, though with more limited durations and ARIs. We use the same digitized versions of TP40 presented in Lopez-Cantu and Samaras (2018) to examine our trend analysis approach in the context of these successive generations of design standards.

2.2. Rainfall Observations

We use daily precipitation observations over CONUS from the Global Historical Climatology Network (GHCN) compiled by NOAA (Menne et al., 2012). We concentrate mainly on changes in rainfall extremes from 1950 to 2017, though we consider two additional periods, as described below. While longer periods are generally preferable for assessing nonstationarity, 1950–2017 corresponds to a period of widespread urbanization and associated expansion of hydrologic infrastructure and the emergence of the National Flood Insurance Program (NFIP) and thus is a logical focus for a study that concentrates on infrastructure-relevant trends.

To ensure interannual homogeneity in our trend analyses, we select GHCN stations with records that are mostly complete (five or fewer missing years of data over the study period; a year is considered "missing" if more than 60 daily precipitation observations are lacking). We aggregate these data to longer durations using a "running sum" approach such that nonoverlapping t-day totals are identified. The approach can identify multiple extremes per year while preventing "double counting" of individual storms.

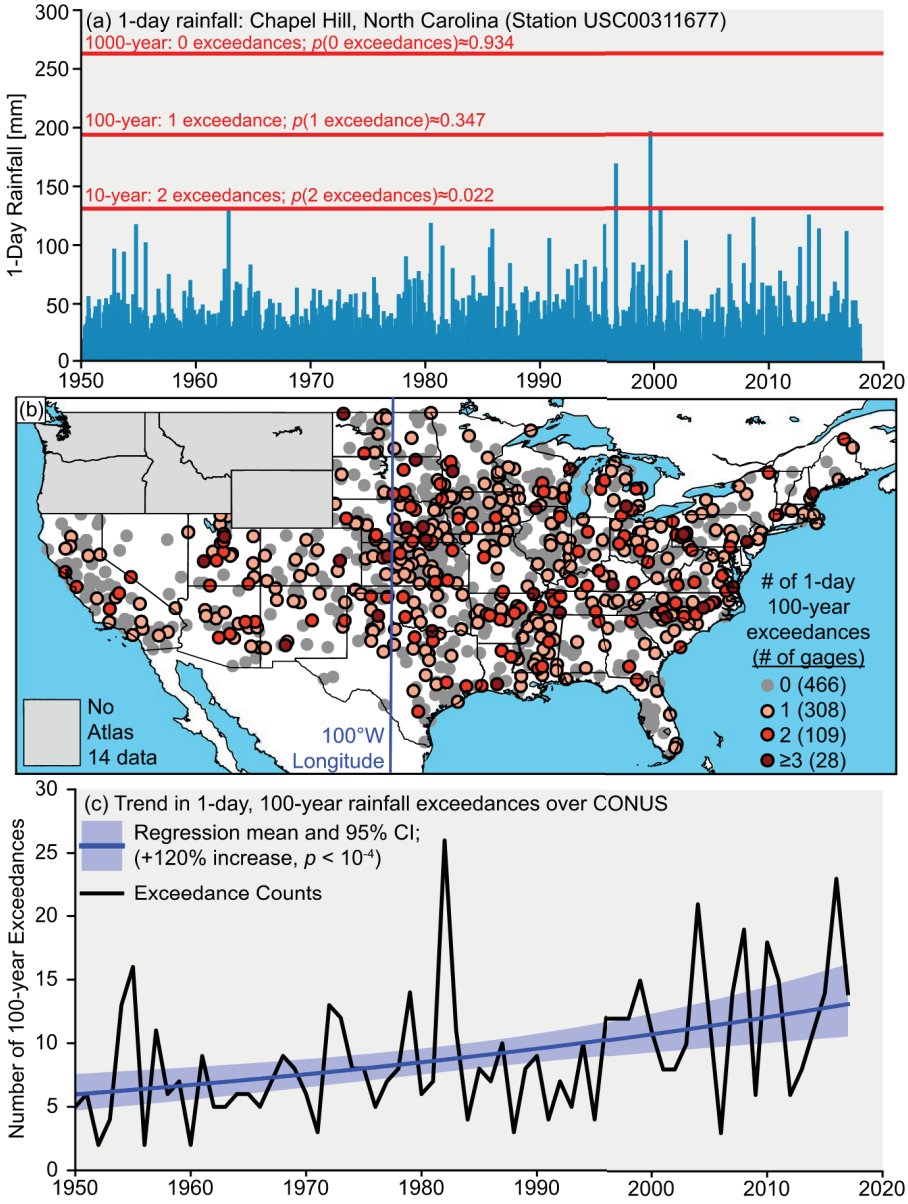

Figure 1. (a) Daily rainfall; 10-, 100-, and 1,000-year intensity-duration-frequency estimates; and exceedances for the one Global Historical Climatology Network station. The probability of the observed number of exceedances is also given, based on the binomial distribution. (b) All Global Historical Climatology Network station locations and total number of 100-year, 24-hr exceedances over the 1950–2017 period. The numbers of gages (out of a total of 911) experiencing given numbers of exceedances is also shown. (c) One-hundred-year, 24-hr, rainfall exceedance counts over all stations shown in (b), and the associated negative binomial regression model. CONUS = conterminous United States.

2.3. Exceedance Counts and Statistical Analyses

We identify instances when GHCN observations exceed IDF estimates (Figures 1a and 1b) for each ARI (1–1,000 years) and duration (24 hr to 7 days). Atlas 14 publishes IDF estimates for 24 and 48 hr, rather than the "calendar" 1- and 2-day durations provided by the GHCN records; the former can be larger than the latter because a rainstorm may straddle two or more calendar days. We use adjustments from Atlas 14 to infer 24-hr rainfalls from daily records; that is, we divide 24-hr IDF estimates by 1.13- and 48-hr estimates by 1.04 prior to identifying exceedances. Though these adjustments are simplifications of the true relationships between extreme precipitation and calendar-day rainfall totals, consistency with Atlas 14 is preferable in this study due to our emphasis on the adequacy of "conventional" IDF estimates. Trends and statistical

significance in sections 3.1 and 3.2 are estimated using negative binomial regression (Hilbe, 2011), which is useful when counts are highly overdispersed (Figure 1c).

2.4. Rainstorm Cluster Identification

A single rainstorm may produce extreme rainfall at more than one location and duration. This can lead to spatial correlation in occurrence counts at a single duration, and potentially to correlation in counts across multiple durations. These correlations may potentially influence the validity of trend tests and potentially complicate inferences regarding the role of climate variability in such trends. We are not aware of statistical methods to account for these effects. An alternative is to identify "clusters" of exceedances that can be reasonably assumed to have been caused by a single storm and conduct analyses on the numbers of clusters, rather than on the numbers of stations that experience exceedances. We identify clusters of 10- and 100-year exceedances using a recursive algorithm:

1. Ten-year exceedances for all durations over a region for a given year are identified. If two or more exceedances of different durations at the same station are concurrent, the longest duration is used for subsequent cluster identification.
2. A 10-year exceedance is selected as the basis for a cluster. All other 10-year exceedances that occurred within 500 km and 1 day of this exceedance are included within the cluster. Then, all remaining 10-year exceedances are reexamined to see if they fall within this 500 km, 1-day range. Once an exceedance has been grouped into a cluster, it cannot be included in another cluster, so that "double counting" is avoided.
3. Each cluster of 10-year exceedances is screened to see if it includes any 100-year exceedances, thus creating two sets of clusters: one based on 10-year exceedances and a subset based on 100-year exceedances. Varying the separation distance from 250–750 km had modest influence on the numbers of 10-year clusters identified but minimal impact on the estimated trend magnitudes and had virtually no impact on the numbers of 100-year clusters (results omitted).

These sets are used as the basis for analyses in section 3.2. Negative binomial regression (section 2.3) is used to assess trends in annual number of clusters and to examine links between these cluster counts and indicators of climate variability. We considered indices of Northern Hemisphere temperature anomalies, multivariate El Niño index (Wolter & Timlin, 2011), detrended Atlantic Multidecadal Oscillation (Kerr, 2000), and Pacific Decadal Oscillation (PDO; Newman et al., 2016) obtained from NOAA. Trend analyses based on annual counts of clusters can be indicative of changes in the frequency of major rainstorms, since each cluster represents one such storm. This is in contrast with results based on exceedance counts, which, due to spatial correlation effects, conflate storm frequency with storm spatial extent.

2.5. Design Versus Observed ARIs

We also examine how our results can inform the reliability of existing IDF estimates. We distinguish between "design ARI," which is fixed, and a time-varying "observed ARI." Design ARI refers to a selected standard, such as the 100-year, 24-hr storm, and will often be prescribed by regulations, such as storm water design standards or the NFIP. Observed ARI is obtained by dividing the total number of observed exceedances of the design ARI by the total number of GHCN gages for that year. Design ARI will often be prescribed by regulations, such as storm water design standards or the NFIP.

In a stationary climate with no IDF estimation error, the long-term average observed ARI should be equal to the design ARI, while time-varying differences suggest temporal nonstationarity. Such systematic differences are highlighted in section 3.3 using a simple moving average smoother (Akaike, 1998). Unlike the aforementioned negative binomial regression, the simple moving average smoother is insensitive to starting date but does not provide a statistical significance level.

3. Results

3.1. Trends in Rainfall Exceedances

Regression results for exceedances of the 24-hr, 100-year rainfall over CONUS suggest that such storms are becoming significantly more frequent since 1950 (Figure 1c). We divide these into two subsets: stations west and east of 100° west longitude (100°W), long-considered a geographic division between the arid Western

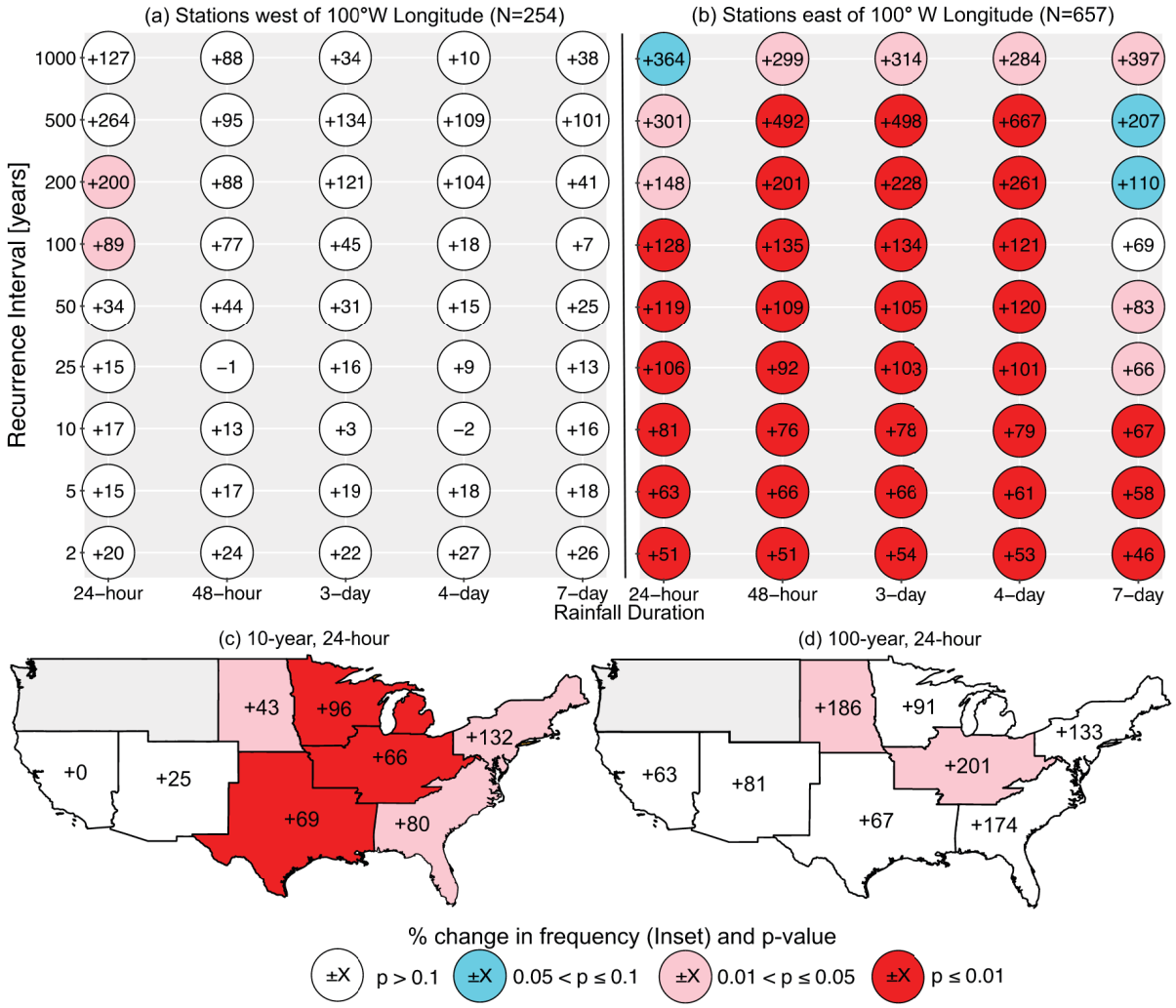

Figure 2. (a) Observed changes (inset values) and regression p values (colors) in frequency of exceedances from 1950 to 2017 for Global Historical Climatology Network stations west of 100°W. (b) Same as (a), but for stations east of 100°W. A change of +100% corresponds to a doubling in frequency. (c) Observed changes (inset values) and regression p values (colors) for the National Oceanic and Atmospheric Administration climate regions for 10-year, 24-hr exceedances. (d) Same as (c), but for 100-year, 24-hr exceedances.

and humid Eastern United States (e.g., Seager et al., 2017). Figures 2a and 2b show statistically significant increases in eastern CONUS, with greater increases at longer ARIs. The frequency of 2-year, 24-hr exceedances, for example, has increased by +51% ($p < 10^{-7}$), but by +301% ($p = 0.012$) for 500-year, 24-hr exceedances. While this pattern generally holds in the west, trends are smaller in magnitude: +20% ($p = 0.15$) and +264% ($p = 0.104$) for 2-year, 24-hr and 500-year, 24-hr exceedances, respectively. These geographic differences are broadly consistent with other studies (e.g., Bonnin, Martin, et al., 2011; Groisman et al., 2001). We also reproduce these analyses for 1930–2017 and 1970–2017 (Figure S1 in the supporting information). While the specific results change when a different starting period is used, the general finding is consistent—increasing frequency of exceedances *east of* 100°W, with smaller and less significant changes farther west.

We repeat these analyses for eight of the NOAA climate regions (e.g., Groisman et al., 2005) to further illustrate regional differences (Figures 2c and 2d; see Figures S2 and S3 for extended results and map of climate regions). Regions in eastern CONUS show significant increases in 10-year, 24-hr exceedances; western regions do not. Frequencies of 100-year, 24-hr exceedances has increased even more but are only significant at the 5% level in the Central and West North Central regions, likely due in part to limited sample sizes.

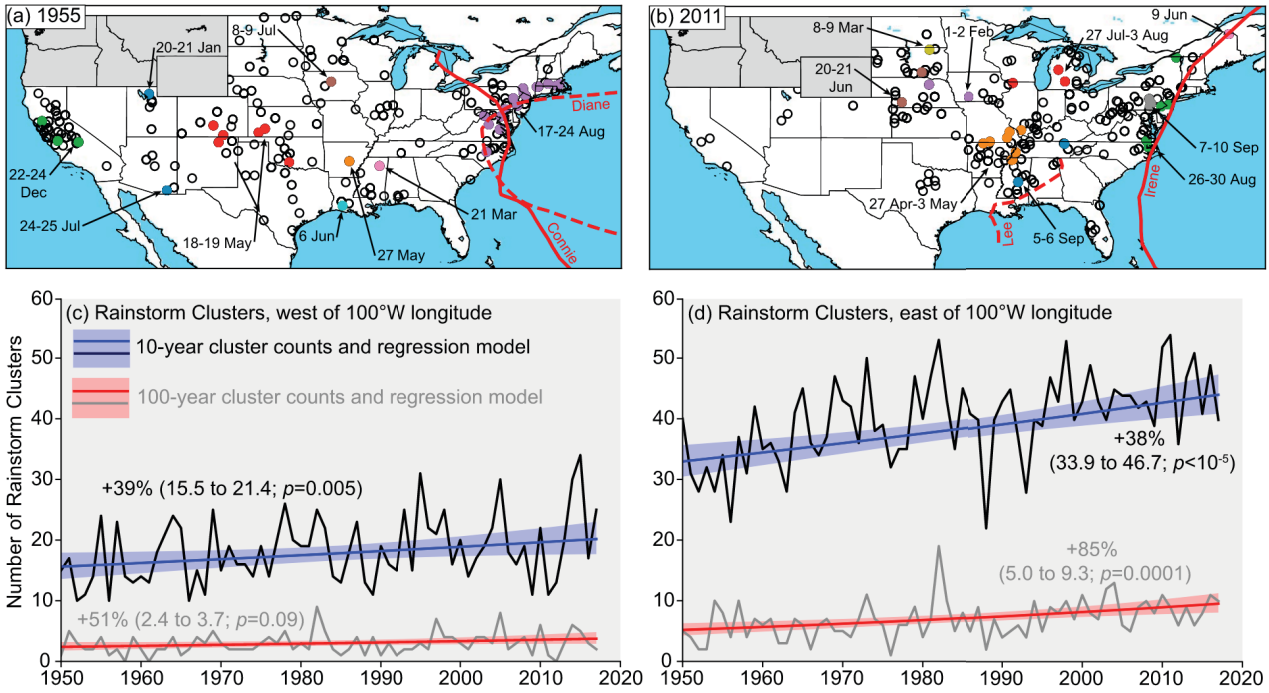

Figure 3. (a) Rainstorm exceedance "clusters" for 1955. Stations with 10-year exceedances of any rainfall duration in 1955 are shown in open circles; 100-year exceedances are colored according to cluster. Landfalling tropical cyclone tracks are also shown. (b) As in (a), but for 2011. (c) Trends in number of 10- and 100-year clusters west of 100°W from 1950 to 2017. (d) As in (c), but for clusters east of 100°W.

3.2. Trends in Rainstorm "Clusters"

Ten-year and 100-year exceedance clusters show considerable interannual variability. For example, 1955 exhibited clusters throughout CONUS, including a cluster resulting from successive hurricanes Connie and Diane (Figure 3a). Year 2011 featured no 100-year clusters in the west but was among the most "active" years in eastern CONUS, including a large cluster associated with Hurricane Irene (Figure 3b). Since 1950, clusters of 100-year exceedances have increased in frequency more than 10-year clusters, with larger and more significant increases in the east (Figures 3c and 3d). This implies that the upward trends in IDF quantile exceedances shown in section 3.1 are likely driven primarily by increased frequency of major storms, though characteristics such as changing storm size or speed cannot be discounted based on our analysis.

We performed regressions on cluster counts for each climate region, using calendar year-averaged Northern Hemisphere temperature anomalies as well as multivariate El Niño index, Atlantic Multidecadal Oscillation,

Table 1
P values for Negative Binomial Regression Models of 10-Year (100-Year) Cluster Counts

	Time	Northern Hemisphere temperature anomalies	ENSO (MEI)	AMO	PDO
Northeast Region	**0.012 (<10^{-4})**	**0.035 (0.003)**	**0.043 (0.463)**	0.329 (0.553)	0.121 (0.111)
Southeast Region	0.057 **(0.033)**	0.173 (0.122)	0.698 (0.903)	0.983 (0.758)	0.897 (0.081)
East North Central Region	**0.005** (0.110)	**0.008** (0.072)	0.100 (0.896)	0.853 (0.529)	0.375 (0.521)
Central Region	**0.002 (0.010)**	**0.039 (0.020)**	0.070 (0.839)	0.399 (0.898)	0.128 (0.540)
South Region	**0.023** (0.201)	0.054 (0.336)	0.484 (0.240)	0.854 (0.840)	0.994 (0.424)
West North Central Region	**0.044** (0.132)	**0.008** (0.168)	0.999 (0.641)	0.113 (0.620)	0.223 (0.672)
Southwest Region	0.105 (0.182)	0.068 (0.068)	0.065 (0.431)	0.599 (0.164)	**0.004** (0.220)
West Region	**0.039** (0.300)	0.073 (0.216)	0.243 (0.962)	0.825 (0.712)	**0.020** (0.765)

Note. ENSO = El Niño-Southern Oscillation; MEI = Multivariate ENSO Index; AMO = Atlantic Multidecadal Oscillation; PDO = Pacific Decadal Oscillation. Values significant at the 5% level are bolded.

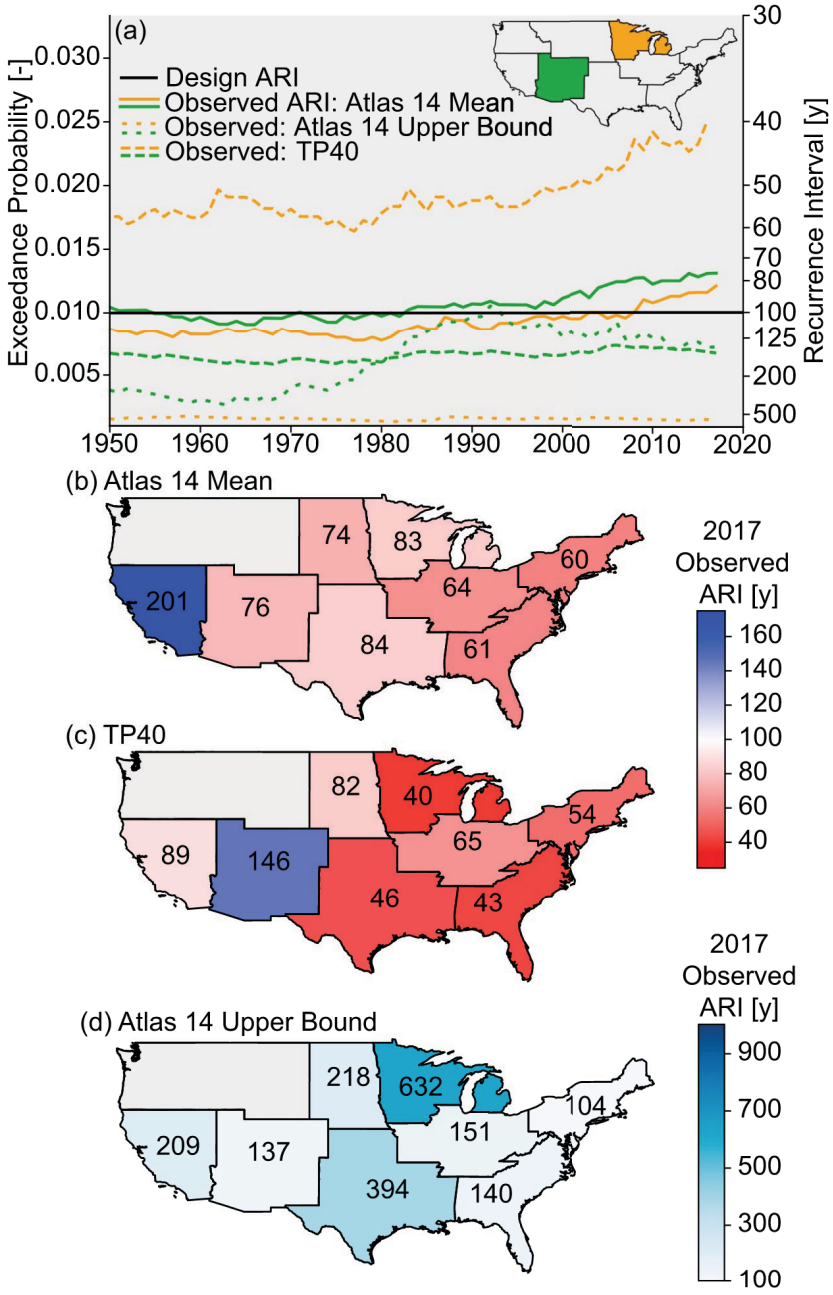

Figure 4. (a) Smoothed time series of 100-year, 24-hr observed annual recurrence interval (ARIs; and their reciprocal, observed exceedance probability) for two National Oceanic and Atmospheric Administration climate regions (see inset map) estimated using the Atlas 14 mean, Atlas 14 confidence interval upper bound, and TP40. (b–d) both inset text and colors show observed ARIs for 2017 for Atlas 14 mean, TP40, and Atlas 14 upper bound, respectively, based on smoothed time series for eight National Oceanic and Atmospheric Administration climate regions. A distinct color scale is used for (d).

and PDO indices as predictors. Statistical significance based upon temperature anomalies was generally akin to those using time for 10-year clusters; results for 100-year clusters exhibited greater variability due to smaller sample sizes (Table 1). PDO was a stronger predictor of 10-year clusters in the Southwest and West than time or temperature, which elsewhere provided higher predictive power than the climate variability indices. These results imply that except in the west and southwestern of the country, secular warming, rather than variability, is the likely driver of observed increases in the frequency of major storms.

3.3. Design Versus Observed ARIs

In section 2.5, we distinguish between design and observed ARI. The former refers to a design standard. A hydrologic structure, for example, may be designed to withstand the flood expected from a 100-year, 24-hr rainfall. The observed ARI in a given year could be different—say 50 (200) years—indicating a doubling (halving) of the likelihood that the structure's design capacity will be exceeded.

The east north central (ENC) and Southwest (SW) climate regions show time-dependent changes in observed ARI of 100-year, 24-hr exceedances estimated based on the Atlas 14 mean and upper bound of the 90% CI, as well on TP40 (Figure 4a). In ENC, observed ARI first dropped below the Atlas 14 mean 100-year estimate (i.e., the design ARI) around 2005, reaching 83 years in 2017. Observed ARI in the SW remained relatively close to the design ARI until about 1980; the 2017 estimate is 76 years. This implies that hydrologic infrastructure in both regions in 2017 designed using the 100-year, 24-hr mean estimate from Atlas 14 would underperform its design standard. Results based on TP40 shows different patterns: in ENC, observed ARI is well below 100 years, decreasing from about 60 years in 1950 to 40 years in 2017. In SW, observed ARI is roughly constant around 150 years. Results based on the upper bound of the Atlas 14 CI also show regional differences: roughly constant around 600 years in ENC; more varied in SW.

We computed 2017 observed ARIs for eight NOAA climate regions using the mean of Atlas 14, as well as TP40 for 100-year, 24-hr rainfall exceedances (Figures 4b and 4c). In 2017, in all regions except West (Southwest), observed ARIs are below 100 years relative to the Atlas 14 mean (TP40) IDF estimates (Figures 4b and 4c). In five regions, observed ARIs based on TP40 are lower than those based on the Atlas 14 mean. We extend this analysis to other durations and recurrence intervals for these eight climate regions for the Atlas 14 mean (Figures S4 and S5) and TP40 (Figure S6). Twenty-four-hour observed ARIs show some of the largest disparities compared with design ARI, which is important since this duration is widely used for infrastructure design. These results suggest that much of hydrologic infrastructure designed using either IDF standard substantially underperforms intended design targets in 2017.

We also use show 2017 observed ARIs for eight NOAA climate regions using the 90% CI upper bound of Atlas 14 100-year, 24-hr IDF estimates (Figure 4d). These observed ARIs are all above the design ARI, though barely (104-year observed ARI) in the case of the Northeastern region. This suggests that using the upper bound of Atlas 14 for design purposes would, at least for 2017 climate conditions, likely ensure compliance with intended design standards.

4. Discussion and Conclusions

We have shown that rainfalls exceeding commonly used IDF design standards are becoming more frequent over much of CONUS since 1950, particularly in the eastern half of the country. This time period coincides with widespread investment in hydrologic infrastructure and floodplain mapping, the reliability of which is called into question due to these rainfall changes. We show that secular climate warming, rather than climate variability, likely explains these increases in most parts of CONUS. We also estimate how the reliability—expressed as a time-varying "observed ARI"—of hydrologic infrastructure or analyses compares with the nominal design ARIs that are used in hydrologic practice. This comparison points to widespread deficiency in much of the existing hydrologic infrastructure and analyses that are based on current and historical IDF standards throughout most of CONUS. This situation will continue to worsen in the future if rainfall extremes intensify further, as is predicted by climate projections.

Our findings differ from those of Bonnin, Martin, et al. (2011), who examined trends in Atlas 14 exceedances in the Southwest and Ohio River basin for 1908–2007. They also showed large changes in exceedances for ARIs less than 25 years, but minimal changes for rarer events. Several methodological differences may explain this discrepancy. They used the Mann-Kendall test (Mann, 1945), which Hodgkins et al. (2017) emphasized is not appropriate given the large numbers of "ties" (oftentimes zeros) that are prevalent in time series of extreme exceedances. The GHCN station network used here is also likely much more extensive than the (unmentioned) number of gages considered in their study.

Our regional aggregation is not without drawbacks. Lopez-Cantu and Samaras (2018) showed that there are substantial differences between IDF estimates from Atlas 14 and TP40 even at the county level. This implies that our regional-scale trend estimates and observed ARIs may not reflect the reality at finer spatial scales.

On the other hand, our approach to estimate observed ARI can inform hydrologic infrastructure reliability assessment techniques that require time-varying exceedance probabilities (e.g., Salas & Obeysekera, 2014). Our study does not consider subdaily precipitation, which is of great importance to infrastructure, particularly in urban areas. Our results at the 24-hr time scale are still relevant to design approaches for such infrastructure, many of which involve disaggregation of 24-hr rainfall totals to finer timescales. Nonetheless, deeper physical understanding of subdaily extremes needed, as both theory (e.g., Trenberth, 2011) and observational and modeling evidence (e.g. Lenderink & van Meijgaard, 2008) suggest that such storms should be more sensitive to climate warming than longer duration events (see Westra et al., 2014).

Despite overwhelming evidence pointing to intensifying rainfall extremes, such changes have not generally translated to clear increases in flood hazard (e.g., Hodgkins et al., 2017). One explanation could be countervailing effects of reductions in soil moisture (Ivancic & Shaw, 2015); changes in rainstorm properties such as storm size or speed also deserve further attention (Chang et al., 2016; Sharma et al., 2018). Drawing conclusions regarding the absence of climate-related flood trends should be done cautiously, in part since previous studies have intentionally excluded the urbanized areas where most infrastructure and people are located and where watershed "carrying capacity" such as soil storage potential is low due to impervious cover and dense storm drain networks.

Our results point to the pressing need to update existing IDF estimates for infrastructure design, floodplain mapping, and other hydrologic analyses. Such updating could potentially make use of nonstationary techniques (e.g., Cheng & AghaKouchak, 2014; Gilleland & Katz, 2016), methods such as stochastic storm transposition that can characterize the current state of the rainfall hydroclimate (Wright et al., 2013; Wright et al., 2017), or use "conservative" estimates such as the upper bound of the 90% CI provided by Atlas 14. Successful updating of such standards will require closer collaboration between climate and hydrologic scientists and the engineering practitioners that are responsible for ensuring our nation's infrastructure reliability.

Acknowledgments
D. B. W.'s and C. D. B.'s efforts were supported by the National Science Foundation Hydrologic Sciences Program (EAR-1749638). T. L.-C.'s contributions were supported by Consejo Nacional de Ciencia y Tecnologia, the National Science Foundation (CMMI-1635638/1635686), and the UCAR Next Generation Fellowship. UCAR is sponsored by the National Science Foundation. We would like to thank the Dr. Simon Michael Papalexiou and an anonymous reviewer for their constructive peer review and Dr. Naresh Devineni for his valuable comments. Data availability: Wright (2019).

References

Akaike, H. (1998). Information theory and an extension of the maximum likelihood principle. In E. Parzen, K. Tanabe, & G. Kitagawa (Eds.), *Selected Papers of Hirotugu Akaike*, (pp. 199–213). New York, NY: Springer. https://doi.org/10.1007/978-1-4612-1694-0_15

Bonnin, G. M., Martin, D., Lin, B., Parzybok, T., Yekta, M., & Riley, D. (2006). *NOAA atlas 14: Precipitation-frequency atlas of the United States*, (Vol. 2). Silver Spring, Maryland: National Weather Service, National Oceanic and Atmospheric Administration.

Bonnin, G. M., Martin, D., Lin, B., Parzybok, T., Yekta, M., & Riley, D. (2011). *NOAA atlas 14: Precipitation-frequency atlas of the United States*, (Vol. 1). Silver Spring, Maryland: National Weather Service, National Oceanic and Atmospheric Administration.

Bonnin, G. M., Maitaria, K., & Yekta, M. (2011). Trends in rainfall exceedances in the observed record in selected areas of the United States. *JAWRA Journal of the American Water Resources Association*, *47*(6), 1173–1182. https://doi.org/10.1111/j.1752-1688.2011.00603.x

Chang, W., Stein, M. L., Wang, J., Kotamarthi, V. R., & Moyer, E. J. (2016). Changes in spatiotemporal precipitation patterns in changing climate conditions. *Journal of Climate*, *29*(23), 8355–8376. https://doi.org/10.1175/JCLI-D-15-0844.1

Cheng, L., & AghaKouchak, A. (2014). Nonstationary precipitation intensity-duration-frequency curves for infrastructure design in a changing climate. *Scientific Reports*, *4*(1), 7093. https://doi.org/10.1038/srep07093

Easterling, D. R., Kunkel, K. E., Arnold, J. R., Knutson, T., LeGrande, A. N., Leung, L. R., et al. (2017). Precipitation change in the United States. In D. J. Wuebbles, D. W. Fahey, K. A. Hibbard, D. J. Dokken, B. C. Stewart, & T. K. Maycock (Eds.), *Climate Science Special Report: Fourth National Climate Assessment*, (Vol. *I*, pp. 207–230). Washington, DC, USA: U.S. Global Change Research Program. https://doi.org/10.7930/J0H993CC

Feng, Z., Leung, L. R., Hagos, S., Houze, R. A., Burleyson, C. D., & Balaguru, K. (2016). More frequent intense and long-lived storms dominate the springtime trend in central US rainfall. *Nature Communications*, *7*(1), 13,429. https://doi.org/10.1038/ncomms13429

Field, C. B., Barros, V., Stocker, T. F., Dahe, Q., Dokken, D. J., Ebi, K. L., Mastrandrea, M. D., Mach, K. J., Plattner, G. K., Allen, S. K., Tignor, M., & Midgley, P. M. (Eds.) (2012). *Managing the risks of extreme events and disasters to advance climate change adaptation: A special report of Working Groups I and II of the Intergovernmental Panel on Climate Change*. Cambridge, UK and New York, USA: Cambridge University Press. https://doi.org/10.1017/CBO9781139177245

Gilleland, E., & Katz, R. W. (2016). extRemes 2.0: An extreme value analysis package in R. *Journal of Statistical Software*, *72*(8), 1–39.

Groisman, P. Y., Knight, R. W., Easterling, D. R., Karl, T. R., Hegerl, G. C., & Razuvaev, V. N. (2005). Trends in intense precipitation in the climate record. *Journal of Climate*, *18*(9), 1326–1350. https://doi.org/10.1175/JCLI3339.1

Groisman, P. Y., Knight, R. W., & Karl, T. R. (2001). Heavy precipitation and high streamflow in the Contiguous United States: Trends in the twentieth century. *Bulletin of the American Meteorologiccl Society*, *82*(2), 219–246. https://doi.org/10.1175/1520-0477(2001)082<0219:HPAHSI>2.3.CO;2

Guilbert, J., Betts, A. K., Rizzo, D. M., Beckage, B., & Bomblies, A. (2015). Characterization of increased persistence and intensity of precipitation in the northeastern United States. *Geophysical Research Letters*, *42*, 1888–1893. https://doi.org/10.1002/2015GL063124

Hershfield, D. M. (1961). *Rainfall frequency atlas of the United States for durations from 30 minutes to 24 hours and return periods from 1-100 years*. Washington, D.C: Weather Bureau, Department of Commerce.

Hilbe, J. M. (2011). *Negative binomial regression*. Cambridge: Cambridge University Press. https://doi.org/10.1017/CBO9780511973420

Hodgkins, G. A., Whitfield, P. H., Burn, D. H., Hannaford, J., Renard, B., Stahl, K., et al. (2017). Climate-driven variability in the occurrence of major floods across North America and Europe. *Journal of Hydrology*, *552*, 704–717. https://doi.org/10.1016/j.jhydrol.2017.07.027

Hosking, J. R. M., & Wallis, J. R. (2005). *Regional frequency analysis: An approach based on L-moments*. Cambridge: Cambridge University Press.

Ivancic, T. J., & Shaw, S. B. (2015). Examining why trends in very heavy precipitation should not be mistaken for trends in very high river discharge. *Climatic Change*, *133*(4), 681–693. https://doi.org/10.1007/s10584-015-1476-1

Kerr, R. A. (2000). A North Atlantic climate pacemaker for the centuries. *Science*, *288*(5473), 1984–1985. https://doi.org/10.1126/science.288.5473.1984

Kunkel, K. E., Andsager, K., & Easterling, D. R. (1999). Long-Term trends in extreme precipitation events over the Conterminous United States and Canada. *Journal of Climate*, *12*(8), 2515–2527. https://doi.org/10.1175/1520-0442(1999)012<2515:LTTIEP>2.0.CO;2

Kunkel, K. E., Easterling, D. R., Kristovich, D. A. R., Gleason, B., Stoecker, L., & Smith, R. (2012). Meteorological causes of the secular variations in observed extreme precipitation events for the conterminous United States. *Journal of Hydrometeorology*, *13*(3), 1131–1141. https://doi.org/10.1175/JHM-D-11-0108.1

Lenderink, G., & van Meijgaard, E. (2008). Increase in hourly precipitation extremes beyond expectations from temperature changes. *Nature Geoscience*, *1*(8), 511–514. https://doi.org/10.1038/ngeo262

Lopez-Cantu, T., & Samaras, C. (2018). Temporal and spatial evaluation of stormwater engineering standards reveals risks and priorities across the United States. *Environmental Research Letters*, *13*(7), 074006. https://doi.org/10.1088/1748-9326/aac696

Mann, H. B. (1945). Non-parametric tests against trend. *Econometrica*, *13*(3), 245–259. https://doi.org/10.2307/1907187

Menne, M. J., Durre, I., Vose, R. S., Gleason, B. E., & Houston, T. G. (2012). An overview of the Global Historical Climatology Network-daily database. *Journal of Atmospheric and Oceanic Technology*, *29*(7), 897–910. https://doi.org/10.1175/JTECH-D-11-00103.1

Milly, P. C. D., Betancourt, J., Falkenmark, M., Hirsch, R. M., Kundzewicz, Z. W., Lettenmaier, D. P., & Stouffer, R. J. (2008). Stationarity is dead: Whither water management? *Science*, *319*(5863), 573–574. https://doi.org/10.1126/science.1151915

Newman, M., Alexander, M. A., Ault, T. R., Cobb, K. M., Deser, C., di Lorenzo, E., et al. (2016). The Pacific Decadal Oscillation, Revisited. *Journal of Climate*, *29*(12), 4399–4427. https://doi.org/10.1175/JCLI-D-15-0508.1

Perica, S., Dietz, S., Heim, S., Hiner, L., Kazungu, M., Martin, D., et al. (2014). *NOAA atlas 14: Precipitation-frequency atlas of the United States*, (Vol. *6*). Silver Spring, Maryland: National Weather Service, National Oceanic and Atmospheric Administration.

Perica, S., Martin, D., Pavlovic, S., Roy, I., St. Laurent, M., Trypaluk, C., et al. (2013a). *NOAA atlas 14: Precipitation-frequency atlas of the United States*, (Vol. *8*). Silver Spring, Maryland: National Weather Service, National Oceanic and Atmospheric Administration.

Perica, S., Martin, D., Pavlovic, S., Roy, I., St. Laurent, M., Trypaluk, C., et al. (2013b). *NOAA atlas 14: Precipitation-frequency atlas of the United States*, (Vol. *9*). Silver Spring, Maryland: National Weather Service, National Oceanic and Atmospheric Administration.

Perica, S., Pavlovic, S., St. Laurent, M., Trypaluk, C., Unruh, D., & Wilhite, O. (2018). *Precipitation-frequency atlas of the United States*, (Vol. 11). Silver Spring, Maryland: National Weather Service, National Oceanic and Atmospheric Administration.

Powell, E. J., & Keim, B. D. (2014). Trends in daily temperature and precipitation extremes for the Southeastern United States: 1948–2012. *Journal of Climate*, *28*(4), 1592–1612. https://doi.org/10.1175/JCLI-D-14-00410.1

Salas, J. D., & Obeysekera, J. (2014). Revisiting the concepts of return period and risk for nonstationary hydrologic extreme events. *Journal of Hydrologic Engineering*, *19*(3), 554–568. https://doi.org/10.1061/(ASCE)HE.1943-5584.0000820

Seager, R., Feldman, J., Lis, N., Ting, M., Williams, A. P., Nakamura, J., et al. (2017). Whither the 100th meridian? The once and future physical and human geography of America's arid–humid divide. Part II: The meridian moves east. *Earth Interactions*, *22*(5), 1–24. https://doi.org/10.1175/EI-D-17-0012.1

Seneviratne, S. I., Nicholls, N., Easterling, D., Goodess, C. M., Kanae, S., Kossin, J., et al. (2012). Changes in climate extremes and their impacts on the natural physical environment. In *Managing the risks of extreme events and disasters to advance climate change adaptation*, (pp. 109–230). Cambridge. Retrieved from: Cambridge University Press. https://ueaeprints.uea.ac.uk/59563/

Serinaldi, F., & Kilsby, C. G. (2015). Stationarity is undead: Uncertainty dominates the distribution of extremes. *Advances in Water Resources*, *77*, 17–36. https://doi.org/10.1016/j.advwatres.2014.12.013

Sharma, A., Wasko, C., & Lettenmaier, D. P. (2018). If precipitation extremes are increasing, why aren't floods? *Water Resources Research*, *54*, 8545–8551. https://doi.org/10.1029/2018WR023749

Trenberth, K. E. (2011). Changes in precipitation with climate change. *Climate Research*, *47*(1), 123–138. https://doi.org/10.3354/cr00953

Westra, S., Fowler, H. J., Evans, J. P., Alexander, L. V., Berg, P., Johnson, F., et al. (2014). Future changes to the intensity and frequency of short-duration extreme rainfall. *Reviews of Geophysics*, *52*, 522–555. https://doi.org/10.1002/2014RG000464

Wolter, K., & Timlin, M. S. (2011). El Niño/Southern Oscillation behaviour since 1871 as diagnosed in an extended multivariate ENSO index (MEI.ext). *International Journal of Climatology*, *31*(7), 1074–1087. https://doi.org/10.1002/joc.2336

Wright, D. B. (2019). Data for "U.S. hydrologic design standards insufficient due to large increases in frequency of rainfall extremes" by Daniel B. Wright, Christopher D. Bosma, Tania Lopez-Cantu in Geophysical Research Letters, 2019., HydroShare. http://www.hydroshare.org/resource/e993565761db45bc86a0b180f219f22a

Wright, D. B., Mantilla, R., & Peters-Lidard, C. D. (2017). A remote sensing-based tool for assessing rainfall-driven hazards. *Environmental Modelling & Software*, *90*, 34–54. https://doi.org/10.1016/j.envsoft.2016.12.006

Wright, D. B., Smith, J. A., Villarini, G., & Baeck, M. L. (2013). Estimating the frequency of extreme rainfall using weather radar and stochastic storm transposition. *Journal of Hydrology*, *488*, 150–165. https://doi.org/10.1016/j.jhydrol.2013.03.003